In-plane valence-band nonparabolicity and anisotropy in strained Si-Ge quantum wells

A. Zaslavsky, T. P. Smith III, D. A. Grützmacher,* S. Y. Lin, and T. O. Sedgwick
IBM Research Division, Thomas J. Watson Research Center, Yorktown Heights, New York 10598

D. A. Syphers
Physics Department, Bowdoin College, Brunswick, Maine 04011
(Received 20 July 1993)

We have observed strong peak shifts in the magnetotunneling $I(V,B_\perp)$ characteristics of strained p-Si/$Si_{1-x}Ge_x$ double-barrier resonant tunneling structures as the transverse field $B_\perp$ orientation is rotated in the sample plane. These peak shifts map out the in-plane anisotropy of the light- and heavy-hole subbands in the Si-Ge well. At large in-plane wave vectors, the heavy- and light-hole $E(k_\perp)$ contours are strongly crimped: the heavy-hole $E(k_\perp)$ is dilated in the $\langle 100 \rangle$ and compressed in the $\langle 110 \rangle$ directions, while the light-hole anisotropy is rotated by 45° with respect to that of the heavy hole. The heavy-hole peak shifts are well described by a simple nonparabolic band model, from which we extract an anisotropic nonparabolicity factor that varies by more than a factor of 2 as a function of crystallographic direction.

The effect of a magnetic field transverse to the tunneling direction ($B_\perp \perp I, I \| z$) on the current-voltage $I(V)$ characteristics of double-barrier resonant tunneling structures (DBRTS's) is well understood. As long as the magnetic length remains larger than the well width, the energies E_i and densities of states of the two-dimensional (2D) subbands in the well are not appreciably changed and the main effect of $B_\perp$ is to modify the energy and transverse momentum conservation rules[1] that govern DBRTS transport. Thus, in a $B_\perp$ field, carriers tunnel from states with energy E and transverse momentum $k_\perp$ in the emitter to states with the same energy but transverse momentum $(k_\perp + \Delta k_\perp)$ in the well, where $\Delta k_\perp = eB_\perp \langle z \rangle / \hbar$ and $\langle z \rangle$ is the distance traversed by tunneling into the well.[2,3] Due to this change in $k_\perp$ conservation, the peak in the supply function $N(V)$—defined as the number of occupied states in the emitter that can tunnel into the well conserving E and $k_\perp$—occurs at higher applied bias, and hence the $I(V)$ peaks shift towards higher V. If the in-plane dispersion $E(k_\perp)$ is parabolic, one obtains immediately that the supply function peak shift is proportional to $B_\perp^2$.[2,4] Since the current into the well depends also on the transmission coefficient of the emitter barrier T_e, which varies with bias, the $B_\perp$-induced shift in the resonant peak bias can deviate from the simple $B_\perp^2$ dependence.[5] Once the variation of T_e with bias is taken into account, $I(V,B_\perp)$ measurements agree very well with the theoretical description, at least in the commonly studied III-V DBRTS.[4,5]

If the in-plane dispersion $E(k_\perp)$ of the tunneling carriers is isotropic, the $B_\perp$-induced shifts of the $I(V,B_\perp)$ peaks obviously cannot depend on the orientation of $B_\perp$ in the sample plane. On the other hand, since the change in the transverse momentum component $\Delta k_\perp$ is both proportional and perpendicular to $B_\perp$, aligning $B_\perp$ to different crystallographic axes of a DBRTS with anisotropic dispersion should reveal the extent of the in-plane band anisotropy. This effect can be understood schematically by referring to Fig. 1(a): if the curvature of the $E(k_\perp)$ dispersion varies along different axes, the supply function $N(V)$ will peak at different values of V. Anisotropy determination by magnetotunneling measurements as a function of $B_\perp$ orientation was originally proposed by Eisenstein *et al.*,[6] but data taken on p-GaAs/$Al_xGa_{1-x}As$ DBRTS (Ref. 7) did not exhibit a strong effect. The first measurements in p-Si/$Si_{1-x}Ge_x$ DBRTS's, where valence-band anisotropies are expected to be stronger than in III-V materials, were reported by Gennser *et al.*,[8] who observed a weak $B_\perp$ orientation dependence in the heavy-hole (HH) $I(V,B_\perp)$ peak and a stronger effect in the light-hole (LH) resonance. In our measurements on superior p-Si/$Si_{1-x}Ge_x$ DBRTS devices of varying well width W, we observe a strong $B_\perp$ orientation dependence in the $I(V,B_\perp)$ characteristics of both the HH_0 and LH_0 resonances. As in Ref. 8 we find that the symmetry axes of the HH_0 and LH_0 bands are rotated by 45°: the constant-$k_\perp$ contour $E(k_\perp)$ of the HH_0 subband is dilated (light mass) along the $\langle 100 \rangle$ and compressed (heavy mass) along the $\langle 110 \rangle$ directions, and *vice versa* for the LH_0 band. We analyze the $I(V,B_\perp)$ shifts of the HH_0 peak within the nonparabolic band model[9] with a single nonparabolicity parameter α and obtain very good agreement by taking α to vary strongly with crystallographic direction.

The strained p-Si/$Si_{1-x}Ge_x$ DBRTS's were grown by atmospheric pressure chemical vapor deposition on Si substrates. The growth sequence and DBRTS parameters have been published elsewhere[10,11] The data reported here were taken on two DBRTS's with $Si_{1-x}Ge_x$ wells ($x=0.25$) of $W=23$ and 35 Å clad by 50-Å Si barriers; for both devices the mean distance between the z coordinates of the hole wave functions in the emitter accumulation layer and the well $\langle z \rangle \approx 95 \pm 10$ Å. The $I(V)$ characteristics of these DBRTS devices at $B_\perp = 0$ are shown in Fig. 1(b). Strong HH_0 and LH_0 resonant peaks with high peak-to-valley ratios are observed in both structures (the

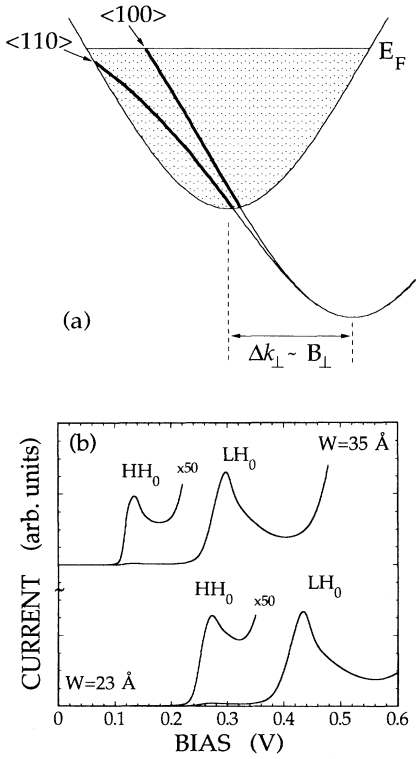

FIG. 1. (a) Schematic diagram of the energy alignment of the occupied heavy-hole states in the emitter (shaded) and the two-dimensional nonparabolic HH_0 subband in the well. The transverse field $B_\perp$ shifts the $k_\perp$-conservation condition by $\Delta k_\perp$. If the nonparabolicity varies with crystallographic direction, as shown, the supply function of hole states that can tunnel elastically (boldface) will vary as a function of $B_\perp$ orientation. (b) $I(V)$ characteristics corresponding to tunneling into the HH_0 and LH_0 subbands of resonant tunneling structures with well widths $W=23$ and 35 Å, at $T=4.2$ K and $B_\perp=0$.

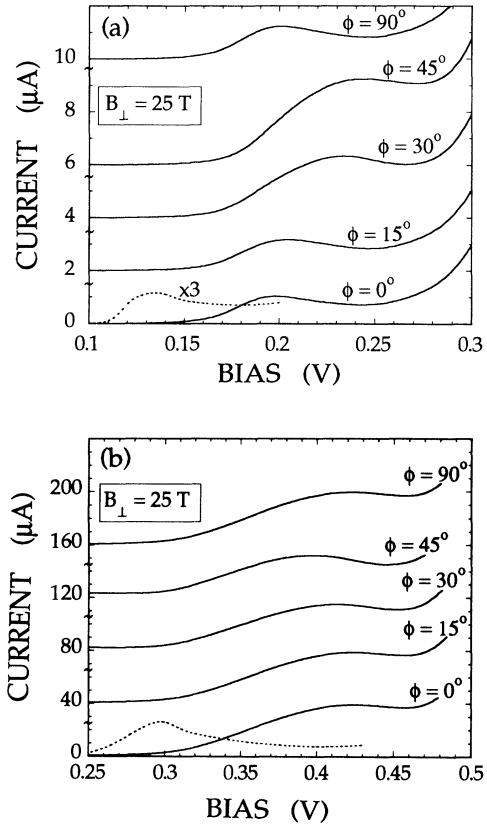

FIG. 2. $I(V,B_\perp)$ characteristics of the $W=35$ Å structure at $B_\perp=25$ T as a function of $B_\perp$ orientation. The HH_0 (a) and LH_0 (b) peaks are shown, ϕ is the angle between $B_\perp$ and the $\langle 110 \rangle$ direction, the dashed line is the $I(V)$ trace at $B_\perp=0$. The $I(V,B_\perp)$ curves are displaced by clarity.

peak assignment is confirmed by calculation of the subband energies and the self-consistent potential distribution over the DBRTS reported previously[11]).

When the DBRTS is placed in a transverse field $B_\perp$, the resonant peaks shift to higher bias and broaden. The magnitude of the peak shift ΔV_p varies with $B_\perp$ orientation in the plane of the sample. Figure 2(a) shows the strong variation in the HH_0 peak shift as a function of angle ϕ between $B_\perp=25$ T and the $\langle 110 \rangle$ direction (wafer cleavage direction in Si) in the $W=35$ Å device, together with the reference $I(V,B_\perp=0)$ trace. Clearly the dependence of ΔV_p on ϕ is very strong: $\Delta V_p \approx 65$ mV when $\phi=0°$ ($B_\perp \| \langle 110 \rangle$), whereas $\Delta V_p \approx 110$ mV when $\phi=45°$ ($B_\perp \| \langle 100 \rangle$). The variation of the LH_0 peak shift in the $W=35$ Å device is shown in Fig. 2(b). The magnitude of the LH_0 peak shift is comparable to the HH_0 result, while the $B_\perp$-induced peak broadening is relatively weaker. The anisotropy follows the crystal symmetry in both heavy- and light-hole subbands, as expected, but with the opposite sign: whenever $B_\perp$ is aligned with the $\langle 100 \rangle$ direction the peak shift ΔV_p is largest for the HH_0 peak and smallest for the LH_0 peak. Hence, for the HH_0 subband the simple geometrical construction in Fig. 1(a) immediately yields the curvature of the in-plane dispersion $E(k_\perp)$ to be steeper along the $\langle 100 \rangle$ direction—in other words, the effective heavy-hole mass m^* away from the $k_\perp=0$ band edge is lighter along the $\langle 100 \rangle$ axis than the $\langle 110 \rangle$ axis.

The $I(V,B_\perp)$ peak-shift measurements for different values of $B_\perp$ in the $W=35$ and 23 Å DBRTS are summarized in Figs. 3(a) and 3(b), respectively. The anisotropic shifts are consistent in the two DBRTS's. The amplitude of the anisotropy varies: for the same $B_\perp=25$ T, the change in HH_0 peak position between $\langle 100 \rangle$ and $\langle 110 \rangle$ $B_\perp$ orientations is larger in the $W=35$ Å structure. However, since $\Delta k_\perp$ is proportional to $\langle z \rangle$ as well as $B_\perp$, and the tunneling current into the well,[5]

$$I(V,B_\perp) \sim eN(V,\Delta k_\perp)T_e(V) \quad (1)$$

varies with the alignment of the 2D subband and the tunneling emitter states through the emitter barrier transmission coefficient T_e, the unequal peak shift anisotropy of Fig. 3 need not directly correspond to different in-plane band anisotropy $E(k_\perp)$. What is clear, however, is that while the peak shift depends strongly on $B_\perp$ orientation, in no way is it proportional to $B_\perp^2$ for any direction

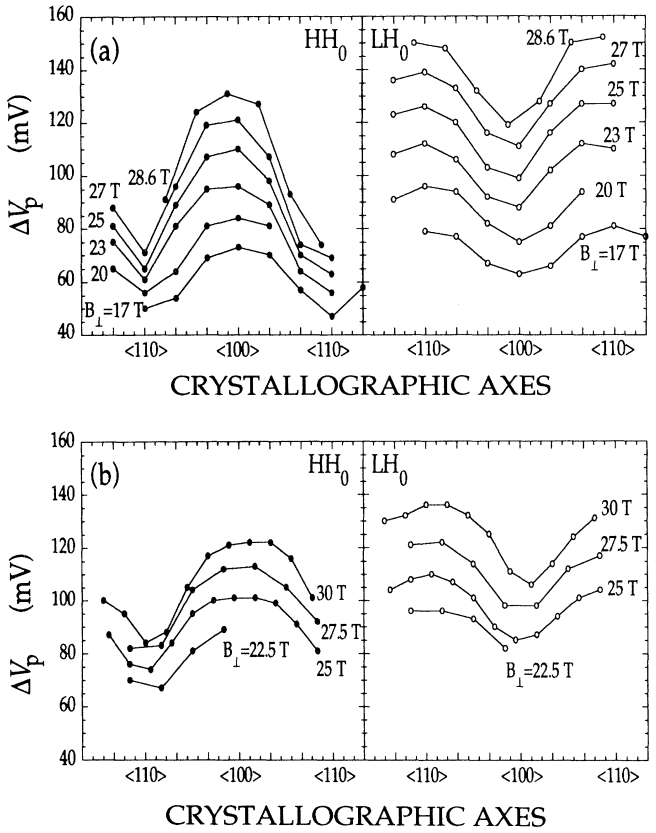

FIG. 3. $B_\perp$-induced peak voltage shifts ΔV_p vs $B_\perp$ magnitude and orientation in the $W=35$ Å (a) and $W=23$ Å (b) structures. Lines connecting the data points are guides to the eye.

of $B_\perp$, indicating that the bands are nonparabolic in all crystallographic directions. We note here that even at the highest $B_\perp$ of our measurements the magnetic length is larger than the well width, so the simple model of Eq. (1) should retain first-order validity.

In order to analyze our $I(V,B_\perp)$ results we must then turn to a nonparabolic dispersion model. Osbourn *et al.* considered a two-band model[9] in which the nonparabolicity is given by the simple analytic expression

$$E(k_\perp)=\hbar^2k_\perp^2/2m^*(k_\perp)=\hbar^2k_\perp^2/2m_0^*(1+\alpha k_\perp^2)\ , \qquad (2)$$

where m_0^* is the in-plane mass at $k_\perp=0$ (estimated from interpolated $Si_{1-x}Ge_x$ band parameters γ_1,γ_2 as $m_0^*=0.13$ for heavy holes) and α is the nonparabolicity factor which for our samples is clearly anisotropic, $\alpha\equiv\alpha(\phi)$. Then, as a function of the single parameter α we fit the $B_\perp$-induced peak shifts of the HH_0 peak as follows: we calculate the potential distribution over the structure self-consistently[12] and estimate the average distance $\langle z\rangle$ traversed by tunneling into the well via the triangular potential approximation for the accumulation layer in the emitter,[13] yielding $\Delta k_\perp$ for a given $B_\perp$ and V. The potential distribution calculation also yields the alignment of the emitter and HH_0 dispersion at bias V and, for a given value of α, the supply function $N(V,\Delta k_\perp)$ is calculated from the geometric construction in Fig. 1(a). Finally, the expected current is calculated from Eq. (1) by integrating the transmission coefficient T_e through the supply function (T_e is evaluated in the WKB approximation with tunneling mass m_z^* obtained from interpolated band parameters).

Analogous calculations on n-GaAs/$Al_xGa_{1-x}As$ DBRTS's,[5] where emitter and subband dispersions were taken as parabolic, gave very good agreement with experimental $I(V,B_\perp)$ line shapes. For the more complicated system at hand the results are summarized in Fig. 4, which shows the experimentally observed HH_0 peak shift $\Delta V_p(B_\perp)$ for $B\geq 8.0$ T (the field at which the anisotropy first becomes discernible) in the $W=35$ Å DBRTS, together with the model results for $\alpha=0$, 3.5×10^{-18} m^2, and 8.5×10^{-18} m^2. Clearly the parabolic band calculation ($\alpha=0$), which exhibits the expected sharp rise in ΔV_p due to the strong $N(V)\sim B_\perp^2$ dependence, does not agree with either the $B\|\langle 100\rangle$ or $B\|\langle 110\rangle$ experimental results. On the other hand, considering the simplicity of the model, the agreement is quite good between the experimental $\Delta V_p(B_\perp)$ for $B_\|\langle 100\rangle,\langle 110\rangle$ and the calculation for $\alpha=3.5\times10^{-18}$ m^2 and 8.5×10^{-18} m^2, respectively [these values of α were actually used to generate the schematic diagram in Fig. 1(a)]. Since the peak shifts $\Delta V_p(B_\perp)$ for an arbitrary $B_\perp$ orientation fall between the $B_\perp\|\langle 100\rangle$ and $\langle 110\rangle$ limits, we have $3.5\leq\alpha(\phi)\leq 8.5\times10^{-18}$ m^2. An analogous calculation for the $W=23$ Å DBRTS yields fairly similar limits on the nonparabolicity factor, $3.0\leq\alpha(\phi)\leq 7.5\times10^{-18}$ m^2. This is not surprising, since in the two-band model[9] that results in Eq. (2) the nonparabolicity factor α is determined by the energy separation $\Delta\varepsilon$ between the two interacting bands, $\alpha\sim 1/\Delta\varepsilon$. From the peak positions shown in Fig. 1(b) and the self-consistent calculation[12,13] we find that the HH_0-LH_0 energy separation in the $W=35$ and 23 Å DBRTS is rather similar at $\sim$55 and $\sim$60 meV, respectively, hence the similar values of $\alpha(\phi)$.

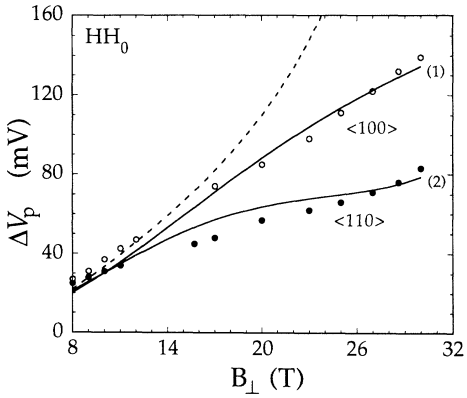

FIG. 4. HH_0 peak voltage shift ΔV_p vs $B_\perp$ oriented along the $\langle 110\rangle$ and $\langle 100\rangle$ directions in the $W=35$ Å structure. Solid lines are ΔV_p values calculated (see text) with the nonparabolicity factor $\alpha=3.5\times10^{-18}$ m^2 (1) and 8.5×10^{-18} m^2 (2); dashed line shows the calculated ΔV_p if the HH_0 subband were parabolic ($\alpha=0$).

We note that these relatively high nonparabolicity factors predict a rapid increase in the in-plane heavy-hole mass from the band-edge value $m_0^* = 0.13$ once $k_\perp$ becomes large: at $k_\perp = 4 \times 10^8$ m^{-1} the effective mass in the $\langle 110 \rangle$ direction is already $m^* \approx 0.31$. While no direct experimental measurements in-plane effective mass along particular crystallographic directions in strained Si-Ge are available, hole cyclotron resonance measurements (which average the effective mass over $k_\perp$ directions) in wide $Si_{1-x}Ge_x$ quantum wells with similar Ge content have yielded values consistent with a heavy in-plane mass at large $k_\perp$.[14]

In principle, the foregoing analysis should be applicable to the light-hole resonances as well, but since the in-plane dispersion of the LH_0 subband can be so strongly nonparabolic as to become electronlike,[15] a geometrical determination of $N(V)$ similar to Fig. 1(a) would require a fairly involved numerical computation[16,17] of the dispersion $E(k_\perp)$ for our strained $Si_{1-x}Ge_x$ quantum-well parameters. Hence we cannot, at this time, describe the LH_0 subband anisotropy of Fig. 3(b) in terms of a single, anisotropic parameter. The remarkably strong anistropy of the heavy-hole subband, however, seems adequately explained by a simple two-band nonparabolic model with the nonparabolicity factor varying by over a factor of 2 between $\langle 100 \rangle$ and $\langle 100 \rangle$ crystallographic directions. A combination of the experimental magnetotunneling data presented in this paper with a more sophisticated calculation of valence-band dispersion in strained $Si_{1-x}Ge_x$ should elucidate the complicated valence-band structure of this scientifically and technologically interesting material.

We are pleased to acknowledge the assistance of C. Roberts, J.-P. Cheng, and the Francis Bitter National Magnet Laboratory staff. Work at IBM was partially supported by ONR (Contract No. N0001492-C-0017).

---

*Present address: Paul Scherrer Institute, Villigen, Switzerland.

[1]S. Luryi, Appl. Phys. Lett **47**, 490 (1985).

[2]L. Eaves, K. W. H. Stevens, and F. W. Sheard, in *The Physics and Fabrication of Microstructures*, edited by M. J. Kelly and C. Weisbuch (Springer-Verlag, New York, 1986), p. 343.

[3]R. A. Davies, D. J. Newson, T. G. Powell, M. J. Kelly, and H. W. Myron, Semicond. Sci. Technol. **2**, 61 (1987).

[4]S. Ben Amor, J. J. L. Rascol, K. P. Martin, R. J. Higgins, R. C. Potter, and H. Hier, Phys. Rev. B **41**, 7860 (1990).

[5]A. Zaslavsky, Yuan P. Li, D. C. Tsui, M. Santos, and M. Shayegan, Phys. Rev. B **42**, 1374 (1990).

[6]J. P. Eisenstein, T. J. Gramila, L. N. Pfeiffer, and K. W. West, Phys. Rev. B **44**, 6511 (1991).

[7]R. K. Hayden, D. K. Maude, L. Eaves, E. C. Valadares, M. Henini, F. W. Sheard, O. H. Hughes, J. C. Portal, and L. Cury, Phys. Rev. Lett. **66**, 1749 (1991).

[8]U. Gennser, V. P. Kesan, D. A. Syphers, T. P. Smith III, S. S. Iyer, and E. S. Yang, Phys. Rev. Lett. **67**, 3828 (1991).

[9]G. C. Osbourn, J. E. Schirber, T. J Drummond, L. R. Dawson, B. L. Doyle, and I. J. Fritz, Appl. Phys. Lett. **49**, 731 (1986).

[10]A. Zaslavsky, D. A. Grützmacher, Y. H. Lee, W. Ziegler, and T O. Sedgwick, Appl. Phys. Lett. **61**, 2872 (1992).

[11]A. Zaslavsky, D. A. Grützmacher, S. Y. Lin, T. P. Smith III, and T. O. Sedgwick, Phys. Rev. B **47**, 1234 (1993).

[12]The HETMOD program, courtesy of A. C. Warren (IBM Research), was used for calculating the potential distribution. The dynamically stored charge density in the well was ignored, as it is small in DBRTS with symmetrical barriers.

[13]T. Ando, A. Fowler, and F. Stern, Rev. Mod. Phys. **54**, 437 (1982).

[14]V. P. Kesan (private communication); see also J.-P. Cheng, V. P. Kesan, D. A. Grützmacher, and T. O. Sedgwick, Appl. Phys. Lett **61**, 2872 (1992).

[15]E. P. O'Reilly and G. P. Witchlow, Phys. Rev. B **34**, 6030 (1986).

[16]L. C. Andreani, A. Pasquarello, and F. Bassani, Phys. Rev. B **36**, 5887 (1987).

[17]R. Winkler and U. Rössler, Phys. Rev. B **48**, 8918 (1993).